Supporting Information

Coordination site manipulation of annular growth mechanism to assemble chiral lanthanide clusters with different shapes and magnetic properties

Bing-Fan Long,[a] Shui Yu,[a] Zhong-Hong Zhu,[a,] Yun-Lan Li,[a] Fu-Pei Liang,[a,b,]* and Hua-Hong Zou[a,]**

[a]School of Chemistry and Pharmaceutical Sciences, State Key Laboratory for Chemistry and Molecular Engineering of Medicinal Resources/Key Laboratory for Chemistry and Molecular Engineering of Medicinal Resources (Ministry of Education of China), Collaborative Innovation Center for Guangxi Ethnic Medicine, School of Chemistry and Pharmaceutical Sciences, Guangxi Normal University, Guilin 541004, P. R. China

[b]Guangxi Key Laboratory of Electrochemical and Magnetochemical Functional Materials, College of Chemistry and Bioengineering, Guilin University of Technology, Guilin 541004, P. R. China

*E-mail (Corresponding author): 18317725515@163.com (Z.-H. Zhu), liangfupei@glut.edu.cn (F.-P. Liang), gxnuchem@foxmail.com (H.-H. Zou).

Keywords: Chiral lanthanide clusters; coordination site; annular growth mechanism; solvothermal synthesis; magnetic properties

Table of Contents:

Figure S13	Temperature-dependent χ' and χ'' AC susceptibilities under 0 Oe dc fields and 1000 Oe dc fields for ***S*-2** (a) and (b).

Experimental Section

Materials and Measurements.

All chemicals and solvents were analytical grade and were used without further purification. The infrared spectra were carried out on a Pekin-Elmer Two spectrophotometer with pressed KBr pellets. The elemental analyses were determined on a Perkin-Elmer model 240 °C elemental analyzer. The powder X-ray diffraction (PXRD) spectra were measured on a Rigaku D/Max-3c diffractometer with Cu-*K*α radiation (λ = 1.5418 Å) and Mo-*K*α radiation (λ = 0.71073 Å). Thermogravimetric analyses were performed on a PerkinElmer Pyris Diamond TG-DTA instrument under an N_2 atmosphere using a heating rate of 5 °C min^{-1} from room temperature up to 1000 °C. The circular dichroism (CD) spectra were recorded on a JASCO J-1500 spectropolarimeter at room temperature. Magnetic properties were performed on a Superconducting Quantum Interference Device (SQUID) magnetometer. The diamagnetism of all constituent atoms was corrected with Pascal's constant.

X-ray crystallography.

Single-crystal X-ray diffraction (SCXRD) data were collected on a ROD, Synergy Custom DW system, HyPix diffractometer (Cu-Kα radiation and λ = 1.54184 Å, Mo-Kα radiation and λ = 0.71073 Å) in Φ and ω scan modes. The structures were solved by direct methods, and refined by a full-matrix least-squares method on the basis of F^2 by using *SHELXL*.[1] Anisotropic thermal parameters were applied to all non-hydrogen atoms. Hydrogen atoms were generated geometrically. Highly disordered free solvent molecules were removed using the SQUEEZE function of PLATON. The crystallographic data for the clusters ***R*-1**, ***S*-1**, ***R*-2** and ***S*-2** are listed in Table S1, and selected bond lengths and angles are given in Table S2−S5. The CCDC reference numbers for the crystal structures of clusters ***R*-1**, ***S*-1**, ***R*-2** and ***S*-2** are 2194449-2194452, respectively.

[1] Sheldrick, G. M. *Acta Crystallogr., Sect. C: Struct. Chem*. **2015**, *71*, 3−8.

The synthesis method.

Synthesis of *R*-1: ***R***-mandelic acid hydrazide (0.1 mmol, 0.0166 g), 2,5-dihydroxybenzaldehyde (0.1 mmol, 0.0138 g), $DyCl_3{\cdot}6H_2O$ (0.5 mmol, 0.1885 g) and triethylamine (30 μL) were dissolved in mixed solvents of methanol (0.8 mL) and water (0.4 mL) in a Pyrex tube. The tube was sealed and heated at 80 °C in an oven for one day, then cooled down slowly, light green block crystals were obtained with a yield of 70% (based on ***R***-mandelic acid hydrazide). Elemental analysis theoretical

value ($C_{130}H_{172}Cl_2Dy_4N_{16}O_{59}$): C, 43.08%; H, 4.78%; N, 6.18%; experimental value: C, 43.01%; H, 4.71%; N, 6.11%. Infrared spectrum data (IR, KBr pellet, cm^{-1}): 3349(s), 1635(s), 1565(s), 1482(s), 1438(s), 1381(s), 1279(s), 1205(s), 1164(m), 1094(w), 1063(m), 955(w), 818(s), 726(m), 695(m), 637(w), 529(w).

Synthesis of *S*-1: The synthesis method was similar to that for ***R*-1** by using ***S***-mandelic acid hydrazide instead of ***R***-mandelic acid hydrazide. The yield is 70% (based on ***S***-mandelic acid hydrazide). Elemental analysis theoretical value ($C_{125}H_{138}Cl_2Dy_4N_{16}O_{49}$): C, 44.56%; H, 4.13%; N, 6.65%; experimental value: C, 44.49%; H, 4.05%; N, 6.58%. Infrared spectrum data (IR, KBr pellet, cm^{-1}): 3368(s), 1628(s), 1561(s), 1484(s), 1438(s), 1381(s), 1273(s), 1203(s), 1164(m), 1090(w), 1066(m), 955(w), 822(s), 733(m), 701(m), 637(w), 529(w).

Synthesis of *R*-2: ***R***-mandelic acid hydrazide (0.1 mmol, 0.0166 g), 2,3,4-trihydroxybenzaldehyde (0.1 mmol, 0.0154 g), $Dy(OAc)_3 \cdot 4H_2O$ (0.5 mmol, 0.2058 g) and triethylamine (30 μL) were dissolved in mixed solvents of methanol (0.8 mL) and water (0.4 mL) in a Pyrex tube. The tube was sealed and heated at 80 °C in an oven for one day, then cooled down slowly, yellow block crystals were obtained with a yield of 65% (based on ***R***-mandelic acid hydrazide). Elemental analysis theoretical value ($C_{71}H_{101}Dy_6N_6O_{49}$): C, 30.48%; H, 3.64%; N, 3.00%; experimental value: C, 30.41%; H, 3.57%; N, 2.95%. Infrared spectrum data (IR, KBr pellet, cm^{-1}): 3400(s), 1565(s), 1447(s), 1279(s), 1197(w), 1063(s), 980(w), 792(w), 742(m), 640(m), 485(w).

Synthesis of *S*-2: The synthesis method was similar to that for ***R*-2** by using ***S***-mandelic acid hydrazide instead of ***R***-mandelic acid hydrazide. The yield is 65% (based on ***S***-mandelic acid hydrazide). Elemental analysis theoretical value ($C_{69}H_{92}Dy_6N_6O_{46}$): C, 30.51%; H, 3.41%; N, 3.09%; experimental value: C, 30.42%; H, 3.33%; N, 3.00%. Infrared spectrum data (IR, KBr pellet, cm^{-1}): 3400(s), 1565(s), 1445(s), 1279(s), 1194(w), 1070(s), 983(w), 790(w), 739(m), 640(m), 481(w).

Table S1. Crystallographic data of the clusters ***R*-1**, ***S*-1**, ***R*-2** and ***S*-2**.

	***R*-1**	***S*-1**	***R*-2**	***S*-2**
Formula	$C_{130}H_{172}Cl_2Dy_4N_{16}O_{59}$	$C_{125}H_{138}Cl_2Dy_4N_{16}O_{49}$	$C_{71}H_{101}Dy_6N_6O_{49}$	$C_{69}H_{92}Dy_6N_6O_{46}$
Formula weight	3623.73	3369.41	2797.57	2716.48
T, K	100.00(10)	100.00(10)	100.00(10)	100.00(10)
Crystal system	orthorhombic	orthorhombic	monoclinic	monoclinic
Space group	$I222$	$I222$	$I2$	$I2$
a, Å	17.8403(2)	21.5282(2)	20.6231(3)	20.6111(5)
b, Å	21.5396(2)	16.8445(2)	21.5982(2)	21.5996(3)
c, Å	16.8287(2)	17.8785(2)	23.8030(4)	23.8049(6)
α, °	90	90	90	90
β, °	90	90	114.7848(19)	114.780(3)
γ, °	90	90	90	90
V, Å^3	6466.81(12)	6483.31(12)	9625.8(3)	9621.9(4)
Z	2	2	4	4
D_c, g cm^{-3}	1.618	1.612	1.747	1.749
μ, mm^{-1}	13.266	13.232	4.678	4.680
F(000)	3140.0	3132.0	4832.0	4836.0
2θ range for data collection/°	6.434 to 151.358	6.426 to 151.798	3.952 to 61.084	4.354 to 61.908
Reflns coll.	22022	22126	77906	48073
Unique reflns	6499	6533	24189	21295
R_{int}	0.0363	0.0330	0.0337	0.0268
R_1[a] ($I > 2\sigma(I)$)	0.0569	0.0546	0.0420	0.0478
wR_2[b] (all data)	0.1580	0.1501	0.1353	0.1344
GOF	1.051	1.046	1.058	1.034
Flack parameter	0.006(3)	0.012(4)	0.029(4)	0.001(5)

[a]$R_1 = \Sigma||F_o|-|F_c||/\Sigma|F_o|$, [b]$wR_2 = [\Sigma w(F_o^2-F_c^2)^2/\Sigma w(F_o^2)^2]^{1/2}$

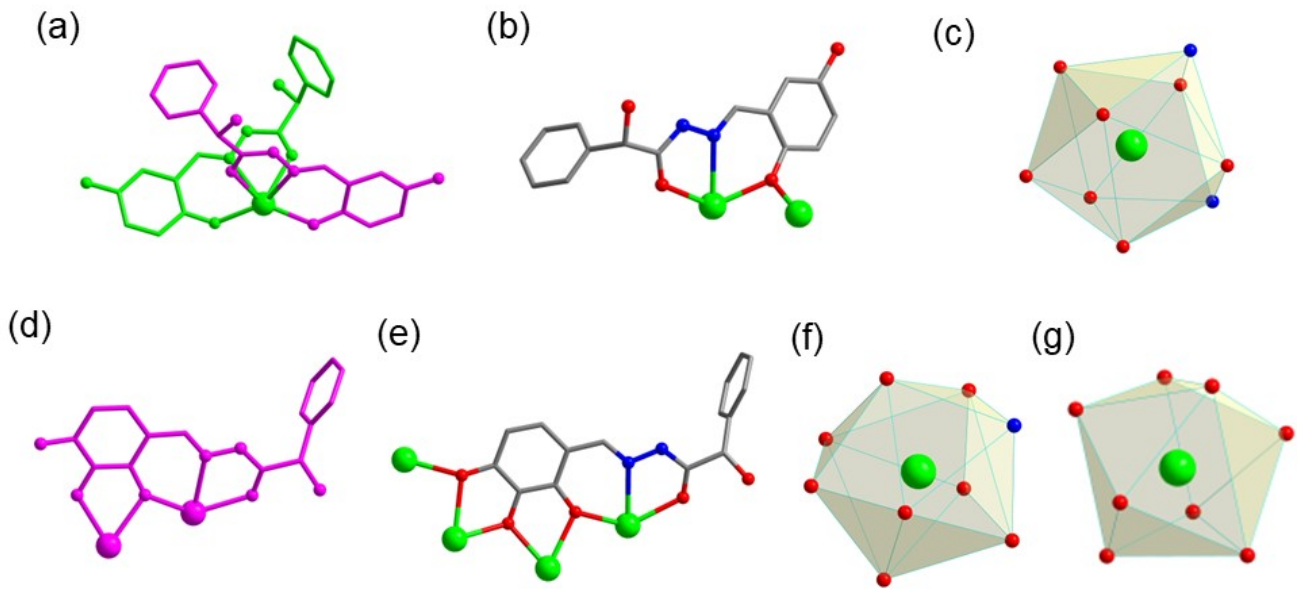

Figure S1. The asymmetric unit of ***S*-1** (a) and ***S*-2** (d); Ligand coordination mode of clusters ***S*-1** (b) and ***S*-2** (e); Coordination polyhedron around the Dy(III) ions of clusters ***S*-1** (c) and ***S*-2** (f and g).

IR spectrum analysis of *R/S*-1 and *R/S*-2.

Specifically, for the ***R*-1** and ***S*-1** the broad absorption peak around 3400 cm^{-1} cans be attributed to the stretching vibration of water molecule ν(HO-H). The strong peak around 1600 cm^{-1}, 1480 cm^{-1} and 1210 cm^{-1} can be attributed to the C=N stretching vibration of the imine group (-C=N-), the stretching vibration of C=N and C=C on the aromatic ring and the stretching vibration between the phenolic hydroxyl groups C-O, respectively. Similarly, for the ***R*-2** and ***S*-2**, the broad absorption peak around 3400 cm^{-1} might be attributed to the stretching vibration of water molecule ν(HO-H). The strong peak around 1560 cm^{-1}, 1450 cm^{-1} and 1200 cm^{-1} might be attributed to the C=N stretching vibration of the imine group (-C=N-), the stretching vibrations of C=N and C=C on the aromatic ring and the stretching vibration between phenolic hydroxyl groups C-O, respectively.

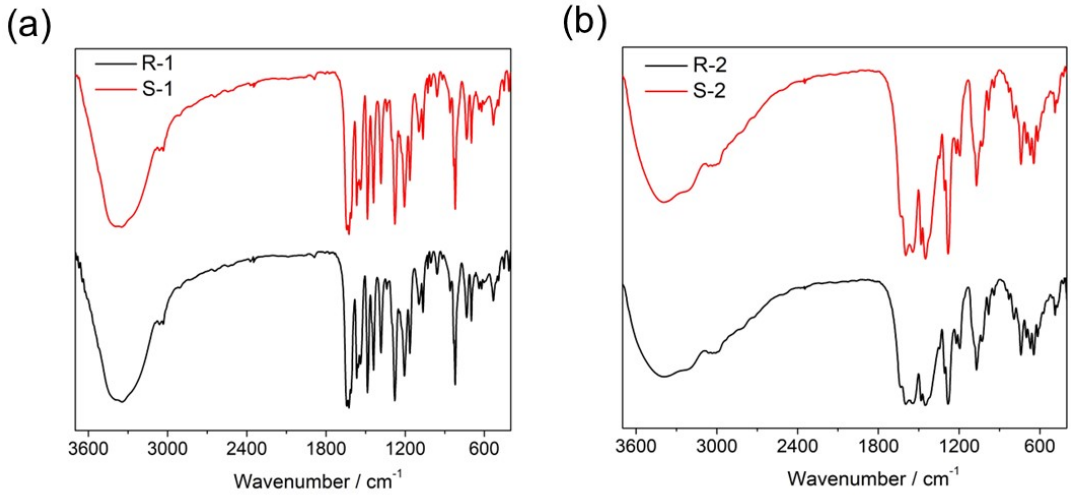

Figure S2. Infrared spectra (IR) of clusters ***R*-1**, ***S*-1**, ***R*-2** and ***S*-2** (a, b).

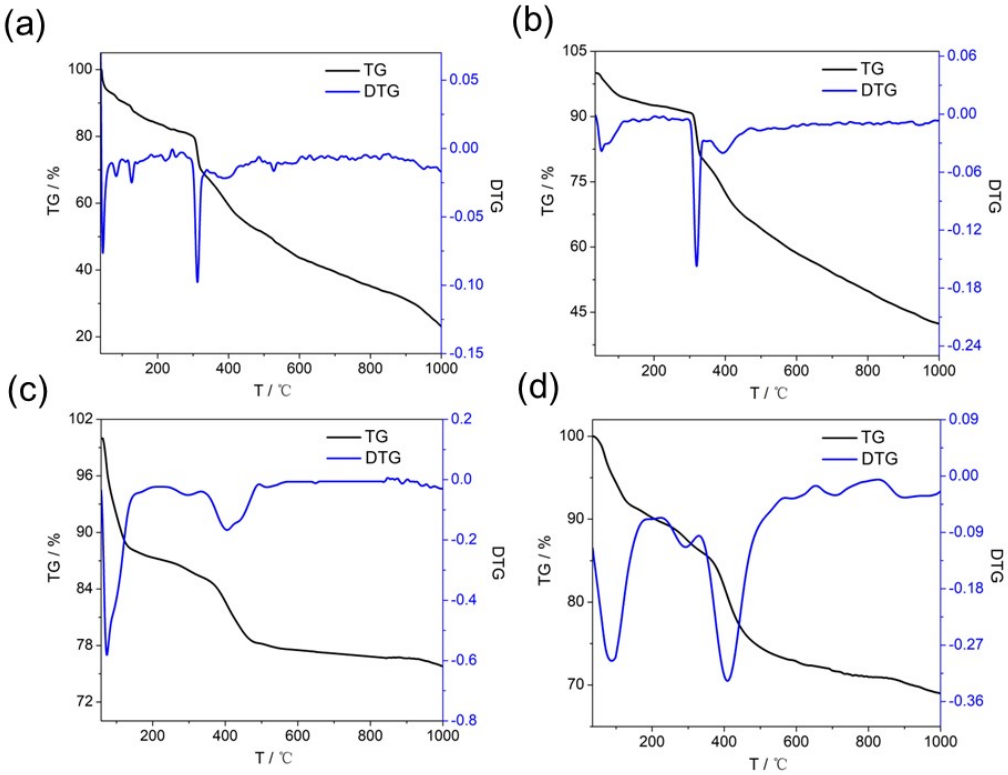

Figure S3. TG curve of clusters ***R*-1**, ***S*-1**, ***R*-2** and ***S*-2** (a-d).

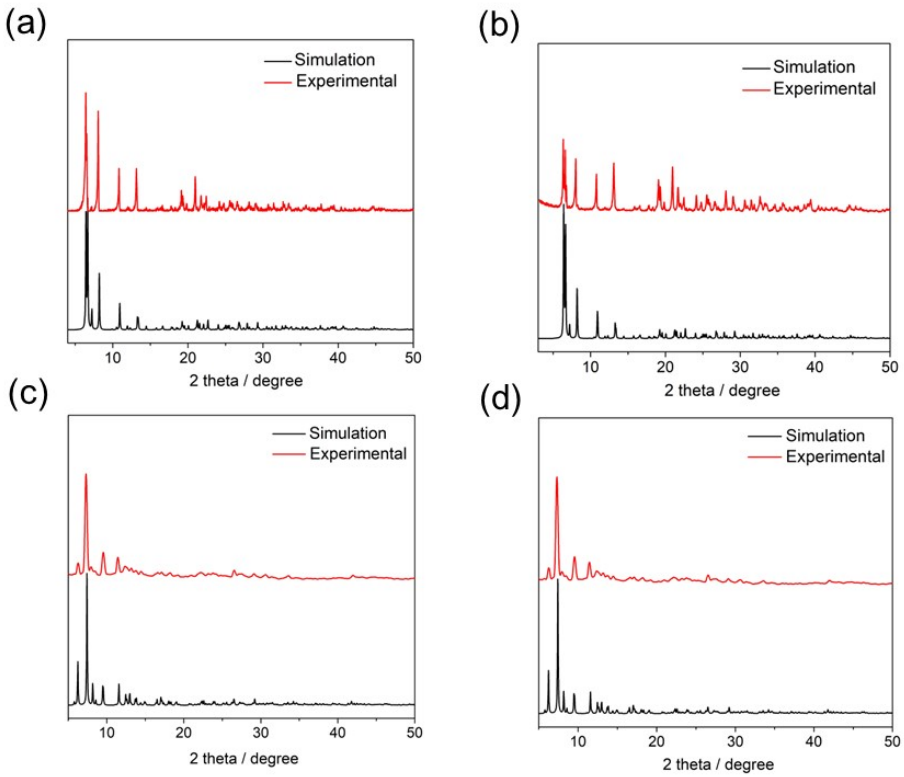

Figure S4. Powder diffraction pattern (PXRD) of clusters ***R*-1**, ***S*-1**, ***R*-2** and ***S*-2** (a-d).

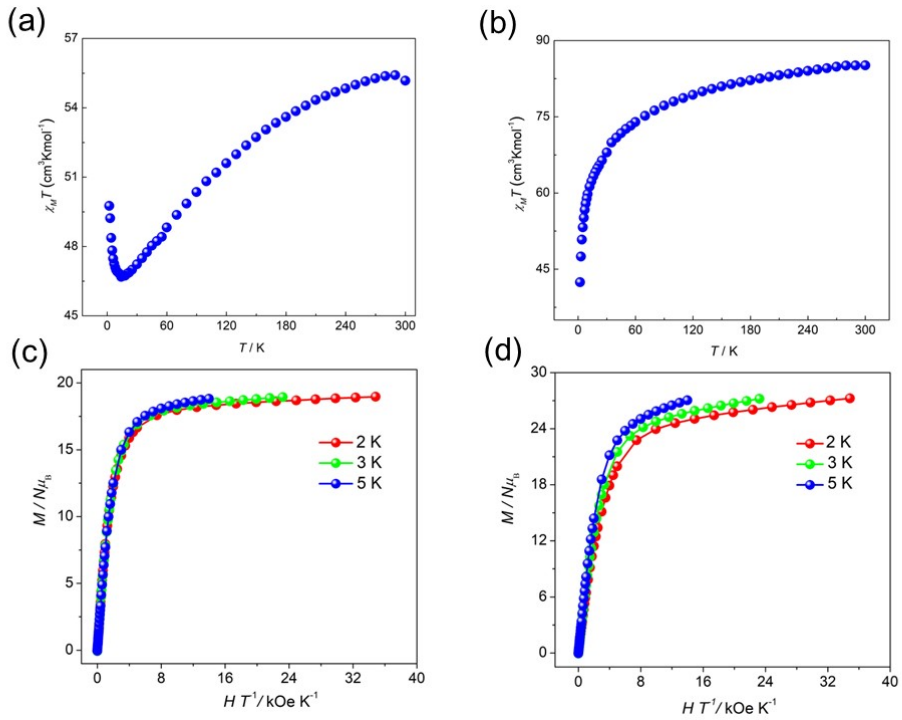

Figure S5. Plots of $\chi_m T$ versus T for clusters ***R*-1** and ***R*-2** (a, b); *M vs. H/T* plots of clusters ***R*-1** and ***R*-2** (c, d).

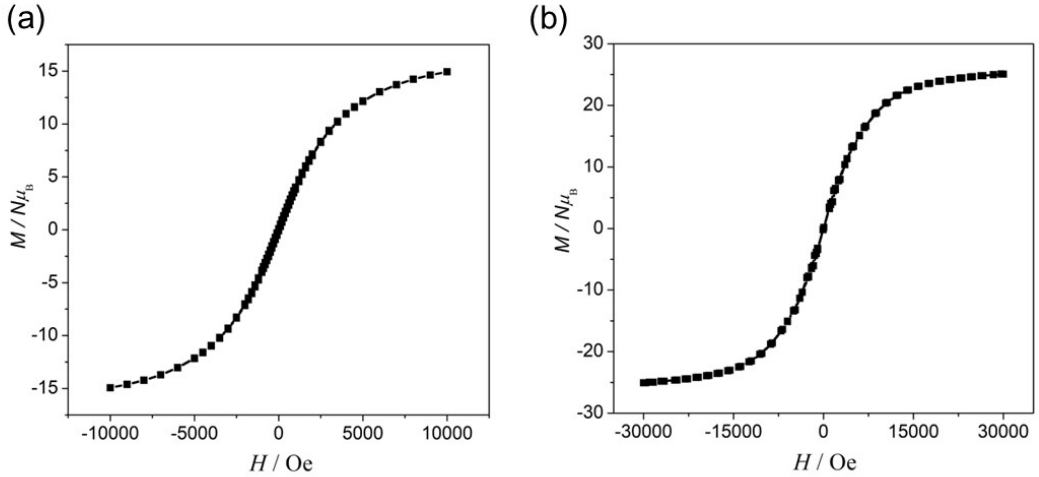

Figure S6. Loop curve graph of clusters ***R*-1** and ***R*-2** (a, b) at 2 K.

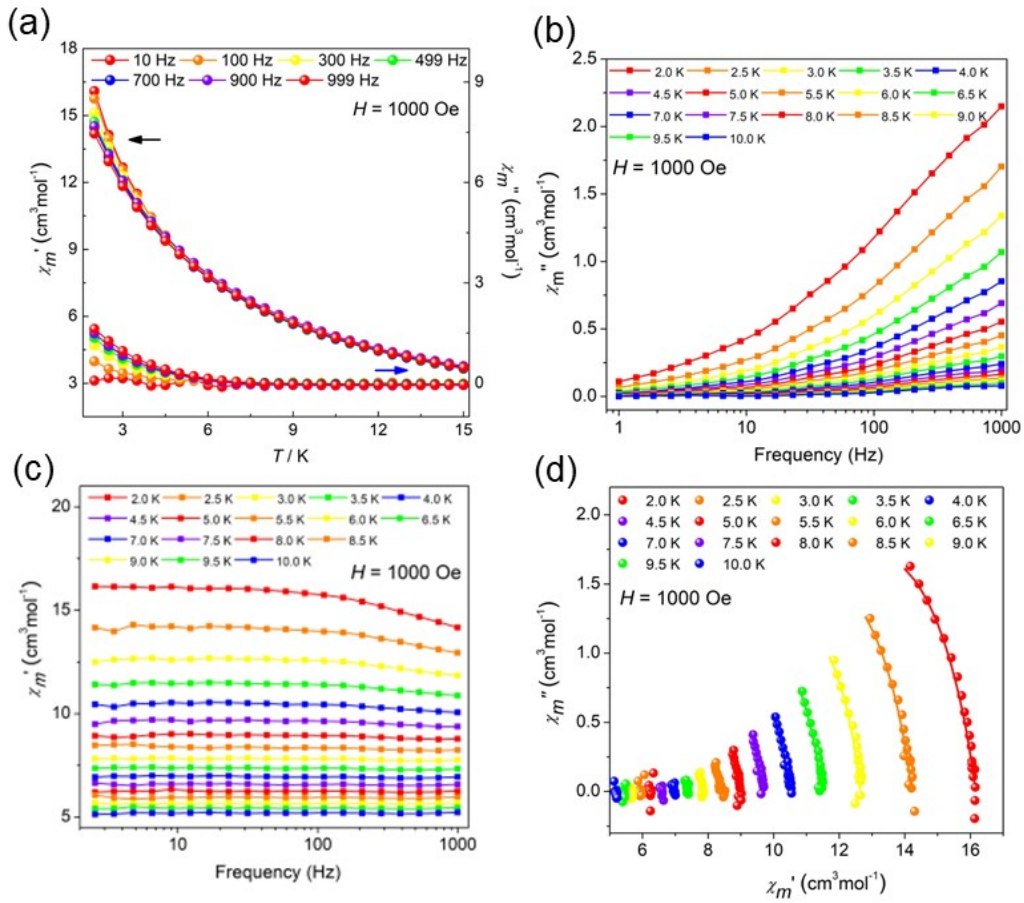

Figure S7. Temperature-dependent χ' and χ'' AC susceptibilities under 1000 Oe DC fields for ***R*-2** (a); Variable-frequency AC susceptibilities (H = 1000 Oe) of cluster ***R*-2** at different temperatures (b and c) and Cole-Cole plots from AC susceptibilities (d).

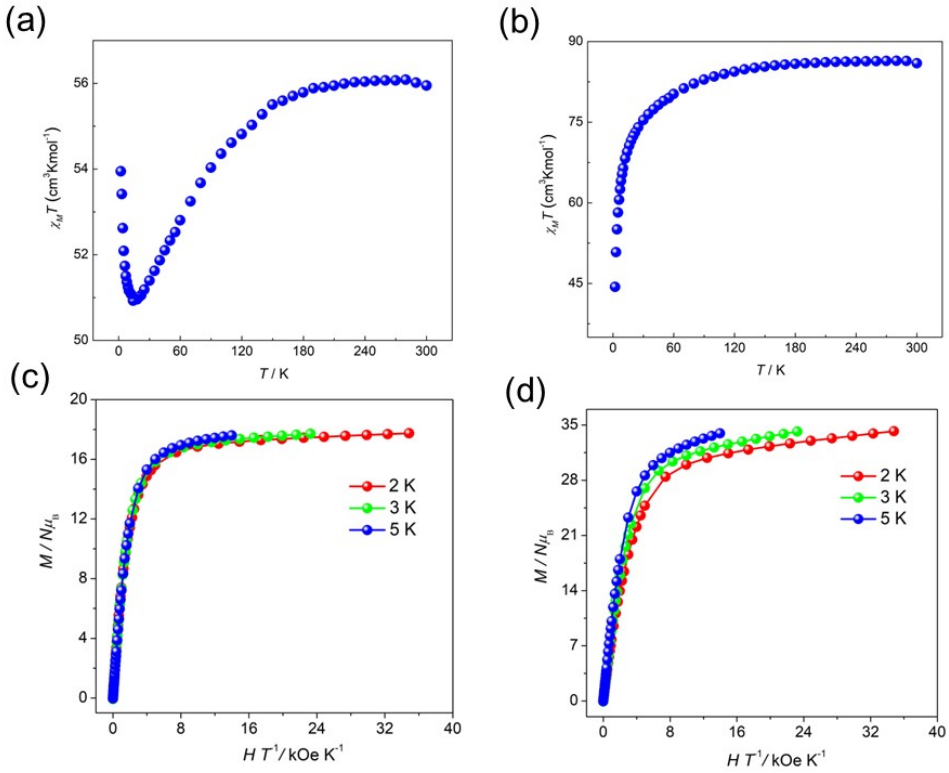

Figure S8. Plots of $\chi_m T$ versus T for clusters ***S*-1** and ***S*-2** (a, b); *M vs. H/T* plots of clusters ***S*-1** and ***S*-2** (c, d).

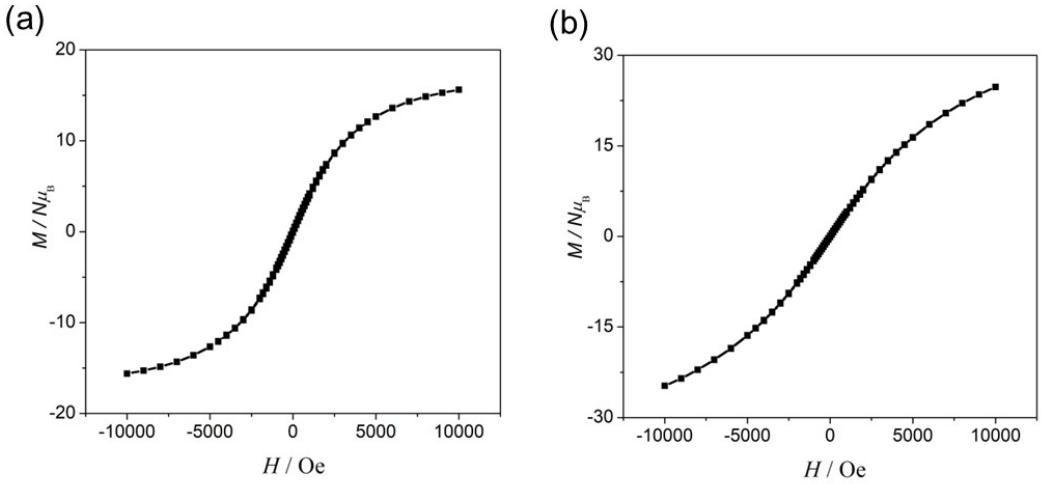

Figure S9. Loop curve graph of clusters ***S*-1** (a) and ***S*-2** (b) at 2 K.

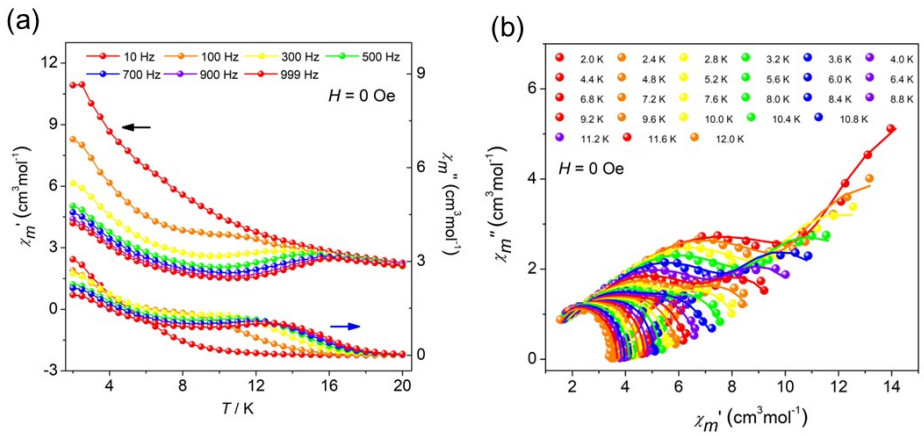

Figure S10. Temperature-dependent χ' and χ'' AC susceptibilities under 0 Oe dc fields for ***S*-1** (a); Cole-Cole plots for ***S*-1** (b).

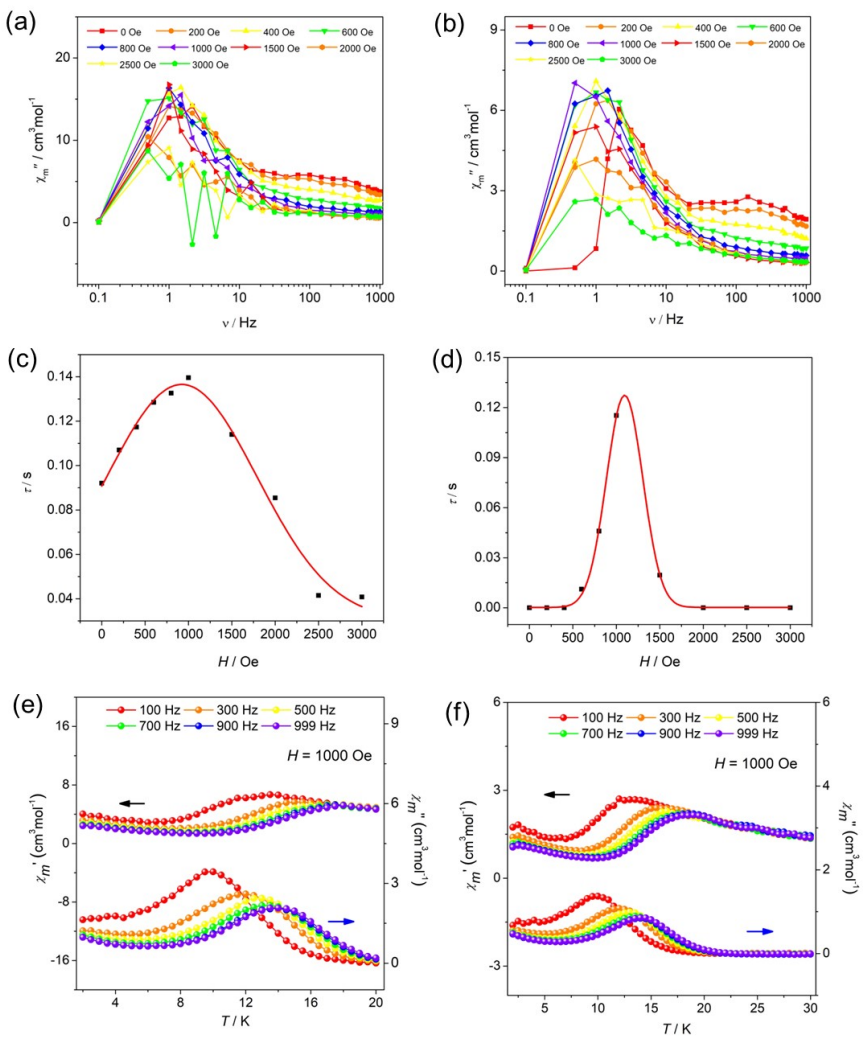

Figure S11. Plots of χ'' *vs.* ν (10−999 Hz) at 2 K under 0−3000 Oe dc field with a 2 Oe oscillating ac field for clusters ***R*-1** (a) and ***S*-1** (b); Field-dependence of the relaxation time (squares) and the best fit curve (red line) for ***R*-1** (c) and ***S*-1** (d); Temperature-dependent χ' and χ'' AC susceptibilities under 1000 Oe dc fields for ***R*-1** (e) and ***S*-1** (f).

Magnetic analysis of cluster *S*-1.

For the ***S*-1**, we applied an Orbach relaxation process ($\tau^{-1} = \tau_0^{-1} \exp(-U_{eff}/k_B T)$ to best fit obtained U_{eff} = 18.64 K, $\tau_0 = 8.5 \times 10^{-5}$ s for the FR phase (Figure S12a); U_{eff} = 30.53 K, $\tau_0 = 1.12 \times 10^{-4}$ s for the SR phase (Figure S12b), respectively. We considered multinomial relaxation processes ($\tau^{-1} = \tau_0^{-1} \exp(-U_{eff}/k_B T) + \tau_{QTM}^{-1} + CT^n$) to fit ***S*-1** over all of the temperature, and we obtained U_{eff} = 28.52 K, $\tau_0 = 6.15 \times 10^{-5}$ s for the FR phase (Figure S12a); U_{eff} = 22.75 K, $\tau_0 = 4.43 \times 10^{-4}$ s for the SR phase (Figure S12b), respectively.

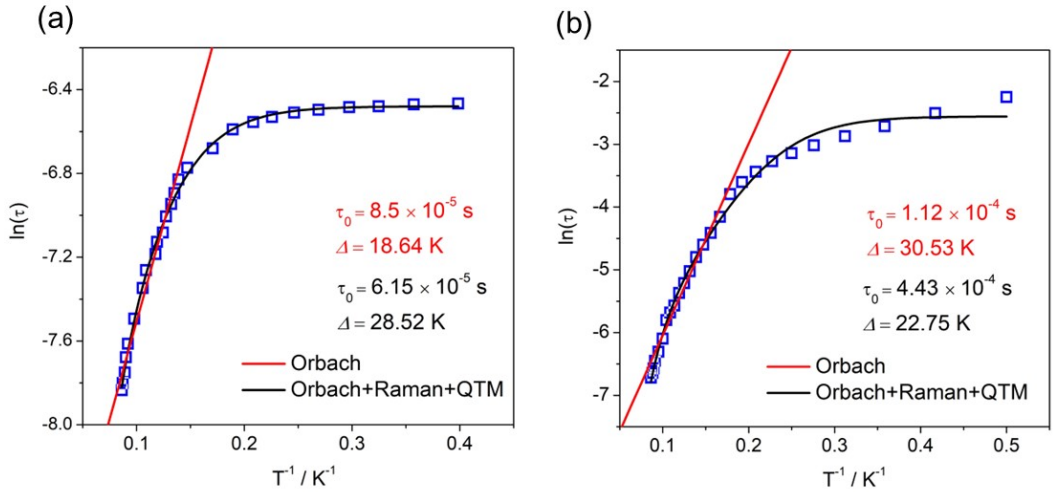

Figure S12. Arrhenius plots generated from the temperature-dependent relaxation times extracted from the Cole-Cole fits of the AC susceptibilities for cluster ***S*-1** under 0 Oe dc field (a and b). Symbols show the extracted times, and the lines are least-squares fits.

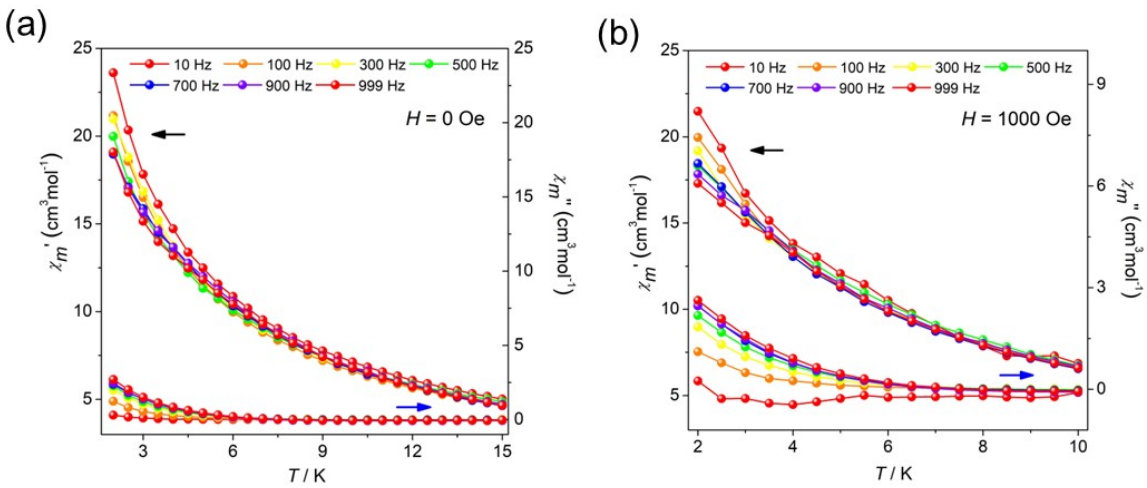

Figure S13. Temperature-dependent χ' and χ'' AC susceptibilities under 0 Oe dc fields and 1000 Oe dc fields for ***S*-2** (a) and (b).

Table S2. Selected bond lengths (Å) and angles (°) of cluster ***R*-1**.

Bond lengths (Å)					
Dy1-O4	2.283(5)	Dy1-O8	2.414(6)	Dy1-O6	2.427(5)
Dy1-O4^{i}	2.419(5)	Dy1-O9	2.5128(3)	Dy1-N4	2.631(7)
Dy1-O8^{ii}	2.309(5)	Dy1-O2	2.402(5)	Dy1-N2	2.653(6)
Bond angles (°)					
O4-Dy1-O4^{i}	76.34(17)	O8-Dy1-O4^{i}	133.55(16)	O9-Dy1-N4	129.37(14)
O4-Dy1-O8	87.40(16)	O8^{ii}-Dy1-O4^{i}	85.91(16)	O9-Dy1-N2	128.61(14)
O4-Dy1-O8^{ii}	137.08(17)	O8^{ii}-Dy1-O8	77.06(17)	O2-Dy1-O4^{i}	75.59(17)
O4-Dy1-O9	68.36(12)	O8^{ii}-Dy1-O9	68.73(13)	O2-Dy1-O8	143.68(17)
O4^{i}-Dy1-O9	66.38(11)	O8-Dy1-O9	67.17(11)	O2-Dy1-O9	134.98(13)
O4-Dy1-O2	125.30(17)	O8^{ii}-Dy1-O2	85.90(19)	O2-Dy1-O6	89.39(17)
O4-Dy1-O6	86.24(18)	O8-Dy1-O6	76.24(17)	O2-Dy1-N4	64.96(19)
O4^{i}-Dy1-O6	143.36(16)	O8^{ii}-Dy1-O6	126.78(17)	O2-Dy1-N2	61.90(18)
O4-Dy1-N4	147.85(19)	O8^{ii}-Dy1-N4	67.81(18)	O6-Dy1-O9	135.62(12)
O4^{i}-Dy1-N4	133.22(18)	O8-Dy1-N4	78.87(18)	O6-Dy1-N4	62.38(18)
O4-Dy1-N2	67.28(17)	O8^{ii}-Dy1-N2	146.88(18)	O6-Dy1-N2	64.45(19)
O4^{i}-Dy1-N2	79.05(17)	O8-Dy1-N2	133.66(17)	N4-Dy1-N2	102.02(19)

Table S3. Selected bond lengths (Å) and angles (°) of cluster ***S*-1**.

Bond lengths (Å)					
Dy1-O4	2.281(5)	Dy1-O8	2.313(5)	Dy1-O6	2.431(5)
Dy1-O4^{ii}	2.424(5)	Dy1-O2	2.399(5)	Dy1-N4	2.620(6)
Dy1-O8^{i}	2.412(5)	Dy1-O9	2.5130(3)	Dy1-N2	2.649(6)
Bond angles (°)					
O4-Dy1-O4^{ii}	76.42(15)	O8^{i}-Dy1-O4^{ii}	133.55(14)	O2-Dy1-O4^{ii}	75.60(16)
O4-Dy1-O8^{i}	87.30(14)	O8-Dy1-O4^{ii}	85.90(14)	O2-Dy1-O8^{i}	143.78(15)
O4-Dy1-O8	137.09(16)	O8-Dy1-O8^{i}	77.09(15)	O2-Dy1-O9	135.03(12)

O4-Dy1-O2	125.20(16)	O8-Dy1-O2	86.08(17)	O2-Dy1-O6	89.22(16)
O4-Dy1-O9	68.43(11)	O8^{i}-Dy1-O9	67.20(11)	O2-Dy1-N4	65.06(17)
O4^{ii}-Dy1-O9	66.35(10)	O8-Dy1-O9	68.67(12)	O2-Dy1-N2	61.77(16)
O4-Dy1-O6	86.29(17)	O8^{i}-Dy1-O6	76.22(16)	O9-Dy1-N4	129.25(13)
O4^{ii}-Dy1-O6	143.42(15)	O8-Dy1-O6	126.69(16)	O9-Dy1-N2	128.74(13)
O4^{ii}-Dy1-N4	133.19(16)	O8-Dy1-N4	67.73(17)	O6-Dy1-O9	135.73(12)
O4-Dy1-N4	147.84(17)	O8^{i}-Dy1-N4	78.86(16)	O6-Dy1-N4	62.35(17)
O4-Dy1-N2	67.31(15)	O8^{i}-Dy1-N2	133.50(16)	O6-Dy1-N2	64.34(18)
O4^{ii}-Dy1-N2	79.22(16)	O8-Dy1-N2	146.97(17)	N4-Dy1-N2	102.01(18)

Table S4. Selected bond lengths (Å) and angles (°) of cluster ***R*-2**.

Bond lengths (Å)					
Dy1-O3	2.232(8)	Dy3-O9	2.263(9)	Dy5-O10	2.274(9)
Dy1-O15	2.299(9)	Dy3-O14	2.312(9)	Dy5-O12	2.356(11)
Dy1-O27	2.356(10)	Dy3-O16	2.345(12)	Dy5-O37	2.365(10)
Dy1-O2	2.370(8)	Dy3-O21	2.352(9)	Dy5-O35	2.420(19)
Dy1-O23	2.435(11)	Dy3-O22	2.393(10)	Dy5-O36	2.433(17)
Dy1-O24	2.465(11)	Dy3-O13	2.402(10)	Dy5-O34	2.488(11)
Dy1-O26	2.493(11)	Dy3-O33	2.414(9)	Dy5-N3	2.551(12)
Dy1-N1	2.563(10)	Dy3-O10	2.458(12)	Dy5-O33	2.623(15)
Dy1-O25	2.604(9)	Dy4-O4	2.258(8)	Dy6-O8	2.236(8)
Dy2-O14	2.253(10)	Dy4-O9	2.326(10)	Dy6-O5	2.292(8)
Dy2-O4	2.303(8)	Dy4-O20	2.333(9)	Dy6-O32	2.347(10)
Dy2-O18	2.328(11)	Dy4-O19	2.349(10)	Dy6-O7	2.400(8)
Dy2-O17	2.331(9)	Dy4-O8	2.387(8)	Dy6-O29	2.451(10)
Dy2-O22	2.399(7)	Dy4-O22	2.389(9)	Dy6-O28	2.452(13)
Dy2-O3	2.410(8)	Dy4-O30	2.412(8)	Dy6-O31	2.497(9)
Dy2-O25	2.419(8)	Dy4-O5	2.464(8)	Dy6-N5	2.567(11)

Dy2-O15	2.467(9)	Dy5-O13	2.236(11)	Dy6-O30	2.608(9)
Bond angles (°)					
O3-Dy1-O15	75.0(3)	O9-Dy3-O14	82.1(3)	O12-Dy5-O35	98.0(7)
O3-Dy1-O27	141.9(4)	O9-Dy3-O16	146.0(4)	O37-Dy5-O35	134.2(6)
O15-Dy1-O27	87.0(4)	O14-Dy3-O16	81.5(4)	O13-Dy5-O36	129.2(5)
O3-Dy1-O2	133.6(3)	O9-Dy3-O21	80.8(3)	O10-Dy5-O36	83.5(5)
O15-Dy1-O2	150.8(3)	O14-Dy3-O21	147.1(4)	O12-Dy5-O36	73.0(5)
O27-Dy1-O2	72.5(3)	O16-Dy3-O21	97.6(5)	O37-Dy5-O36	81.3(6)
O3-Dy1-O23	79.2(4)	O9-Dy3-O22	70.5(3)	O35-Dy5-O36	53.6(6)
O15-Dy1-O23	80.6(4)	O14-Dy3-O22	69.4(3)	O13-Dy5-O34	80.2(4)
O27-Dy1-O23	131.3(5)	O16-Dy3-O22	75.9(4)	O10-Dy5-O34	118.8(4)
O2-Dy1-O23	97.3(4)	O21-Dy3-O22	78.5(3)	O12-Dy5-O34	78.0(5)
O3-Dy1-O24	130.0(4)	O9-Dy3-O13	111.1(3)	O37-Dy5-O34	79.4(4)
O15-Dy1-O24	83.8(3)	O14-Dy3-O13	68.0(3)	O35-Dy5-O34	144.1(5)
O27-Dy1-O24	79.3(4)	O16-Dy3-O13	89.8(5)	O36-Dy5-O34	148.8(4)
O2-Dy1-O24	72.3(3)	O21-Dy3-O13	144.8(4)	O13-Dy5-N3	70.8(4)
O23-Dy1-O24	52.7(5)	O22-Dy3-O13	136.5(3)	O10-Dy5-N3	141.1(4)
O3-Dy1-O26	80.5(3)	O9-Dy3-O33	133.2(4)	O12-Dy5-N3	65.1(4)
O15-Dy1-O26	118.6(4)	O14-Dy3-O33	131.1(3)	O37-Dy5-N3	133.2(4)
O27-Dy1-O26	79.2(4)	O16-Dy3-O33	78.8(4)	O35-Dy5-N3	73.6(5)
O2-Dy1-O26	78.5(3)	O21-Dy3-O33	80.0(4)	O36-Dy5-N3	104.6(6)
O23-Dy1-O26	147.0(4)	O22-Dy3-O33	144.1(4)	O34-Dy5-N3	72.5(4)
O24-Dy1-O26	147.9(3)	O13-Dy3-O33	67.7(4)	O13-Dy5-O33	66.5(4)
O3-Dy1-N1	70.4(3)	O9-Dy3-O10	68.0(3)	O10-Dy5-O33	68.0(4)
O15-Dy1-N1	141.1(3)	O14-Dy3-O10	111.8(4)	O12-Dy5-O33	122.7(5)
O27-Dy1-N1	131.6(3)	O16-Dy3-O10	145.9(4)	O37-Dy5-O33	73.6(4)
O2-Dy1-N1	64.0(3)	O21-Dy3-O10	87.2(4)	O35-Dy5-O33	138.0(6)
O23-Dy1-N1	76.1(4)	O22-Dy3-O10	137.8(3)	O36-Dy5-O33	143.1(5)

O24-Dy1-N1	105.3(4)	O13-Dy3-O10	68.6(4)	O34-Dy5-O33	50.8(3)
O26-Dy1-N1	72.7(3)	O33-Dy3-O10	68.8(4)	N3-Dy5-O33	112.3(4)
O3-Dy1-O25	67.4(3)	O4-Dy4-O9	82.3(3)	O8-Dy6-O5	74.0(3)
O15-Dy1-O25	68.0(3)	O4-Dy4-O20	147.1(3)	O8-Dy6-O32	140.6(3)
O27-Dy1-O25	74.8(3)	O9-Dy4-O20	80.0(3)	O5-Dy6-O32	86.0(4)
O2-Dy1-O25	123.4(3)	O4-Dy4-O19	82.5(3)	O8-Dy6-O7	133.9(3)
O23-Dy1-O25	138.6(4)	O9-Dy4-O19	146.5(3)	O5-Dy6-O7	151.7(3)
O24-Dy1-O25	142.2(3)	O20-Dy4-O19	97.5(4)	O32-Dy6-O7	73.6(4)
O26-Dy1-O25	50.6(3)	O4-Dy4-O8	112.2(3)	O8-Dy6-O29	129.9(4)
N1-Dy1-O25	112.4(3)	O9-Dy4-O8	68.1(3)	O5-Dy6-O29	84.3(3)
O14-Dy2-O4	82.6(3)	O20-Dy4-O8	86.3(3)	O32-Dy6-O29	79.6(4)
O14-Dy2-O18	146.1(3)	O19-Dy4-O8	145.4(3)	O7-Dy6-O29	73.0(3)
O4-Dy2-O18	80.5(3)	O4-Dy4-O22	70.2(3)	O8-Dy6-O28	79.5(4)
O14-Dy2-O17	82.6(4)	O9-Dy4-O22	69.6(3)	O5-Dy6-O28	83.5(4)
O4-Dy2-O17	145.9(3)	O20-Dy4-O22	77.6(3)	O32-Dy6-O28	132.3(4)
O18-Dy2-O17	95.4(4)	O19-Dy4-O22	77.2(3)	O7-Dy6-O28	95.7(4)
O14-Dy2-O22	70.2(3)	O8-Dy4-O22	136.6(3)	O29-Dy6-O28	53.2(5)
O4-Dy2-O22	69.3(3)	O4-Dy4-O30	133.2(3)	O8-Dy6-O31	81.2(3)
O18-Dy2-O22	76.4(4)	O9-Dy4-O30	132.4(3)	O5-Dy6-O31	119.6(3)
O17-Dy2-O22	76.8(3)	O20-Dy4-O30	78.0(3)	O32-Dy6-O31	79.8(3)
O14-Dy2-O3	111.6(3)	O19-Dy4-O30	78.3(3)	O7-Dy6-O31	76.6(3)
O4-Dy2-O3	67.9(3)	O8-Dy4-O30	68.8(3)	O29-Dy6-O31	147.0(3)
O18-Dy2-O3	88.8(4)	O22-Dy4-O30	142.6(3)	O28-Dy6-O31	144.0(4)
O17-Dy2-O3	146.1(3)	O4-Dy4-O5	68.8(3)	O8-Dy6-N5	70.8(3)
O22-Dy2-O3	136.5(3)	O9-Dy4-O5	111.3(3)	O5-Dy6-N5	139.9(3)
O14-Dy2-O25	132.7(3)	O20-Dy4-O5	143.9(3)	O32-Dy6-N5	133.8(4)
O4-Dy2-O25	131.5(3)	O19-Dy4-O5	90.4(3)	O7-Dy6-N5	64.3(3)
O18-Dy2-O25	79.3(3)	O8-Dy4-O5	68.3(3)	O29-Dy6-N5	104.2(4)

O17-Dy2-O25	79.8(3)	O22-Dy4-O5	138.4(2)	O28-Dy6-N5	72.0(5)
O22-Dy2-O25	144.2(3)	O30-Dy4-O5	69.2(3)	O31-Dy6-N5	73.1(3)
O3-Dy2-O25	68.0(3)	O13-Dy5-O10	74.8(4)	O8-Dy6-O30	67.6(3)
O14-Dy2-O15	68.1(3)	O13-Dy5-O12	134.8(4)	O5-Dy6-O30	68.5(3)
O4-Dy2-O15	112.1(3)	O10-Dy5-O12	150.0(4)	O32-Dy6-O30	73.6(3)
O18-Dy2-O15	145.8(3)	O13-Dy5-O37	139.7(5)	O7-Dy6-O30	121.8(3)
O17-Dy2-O15	90.3(4)	O10-Dy5-O37	85.3(4)	O29-Dy6-O30	142.6(3)
O22-Dy2-O15	137.5(3)	O12-Dy5-O37	73.1(4)	O28-Dy6-O30	141.2(4)
O3-Dy2-O15	68.9(3)	O13-Dy5-O35	78.0(6)	O31-Dy6-O30	51.1(3)
O25-Dy2-O15	68.6(3)	O10-Dy5-O35	82.1(6)	N5-Dy6-O30	113.2(3)

Table S5. Selected bond lengths (Å) and angles (°) of cluster ***S*-2**.

Bond lengths (Å)					
Dy1-O15	2.299(10)	Dy3-O29	2.415(8)	Dy5-O8	2.241(8)
Dy1-O23	2.620(10)	Dy3-O9	2.319(10)	Dy5-O30	2.440(14)
Dy1-O3	2.240(9)	Dy3-O21	2.332(10)	Dy5-O5	2.290(9)
Dy1-O25	2.436(12)	Dy3-O8	2.390(9)	Dy5-O32	2.343(11)
Dy1-O24	2.483(11)	Dy3-O22	2.382(9)	Dy5-O7	2.386(9)
Dy1-O26	2.458(12)	Dy3-O4	2.257(9)	Dy5-O31	2.459(11)
Dy1-O2	2.374(8)	Dy3-O16	2.351(11)	Dy5-N3	2.571(11)
Dy1-O27	2.352(10)	Dy3-O5	2.456(9)	Dy5-O28	2.487(10)
Dy1-N2	2.565(11)	Dy4-O14	2.311(10)	Dy6-O12	2.357(12)
Dy2-O17	2.340(11)	Dy4-O9	2.261(10)	Dy6-O13	2.223(11)
Dy2-O14	2.244(10)	Dy4-O13	2.411(11)	Dy6-O10	2.279(10)
Dy2-O15	2.467(11)	Dy4-O22	2.392(11)	Dy6-O33	2.482(12)
Dy2-O22	2.395(7)	Dy4-O10	2.457(13)	Dy6-O37	2.355(11)
Dy2-O4	2.309(9)	Dy4-O19	2.353(13)	Dy6-O34	2.633(15)
Dy2-O23	2.408(8)	Dy4-O20	2.357(11)	Dy6-O36	2.423(17)

Dy2-O3	2.405(9)	Dy4-O34	2.416(10)	Dy6-N5	2.548(12)
Dy2-O18	2.332(11)	Dy5-O29	2.596(10)	Dy6-O35	2.437(19)
Bond angles (°)					
O15-Dy1-O23	67.6(4)	O29-Dy3-O5	68.8(3)	O30-Dy5-O29	141.5(4)
O15-Dy1-O25	81.4(5)	O9-Dy3-O29	132.7(3)	O30-Dy5-O31	52.9(5)
O15-Dy1-O24	118.1(4)	O9-Dy3-O21	79.8(3)	O30-Dy5-N3	72.2(5)
O15-Dy1-O26	83.8(4)	O9-Dy3-O8	68.3(3)	O30-Dy5-O28	144.2(5)
O15-Dy1-O2	150.7(3)	O9-Dy3-O22	69.3(3)	O5-Dy5-O29	68.2(3)
O15-Dy1-O27	86.4(4)	O9-Dy3-O16	146.2(3)	O5-Dy5-O30	83.8(5)
O15-Dy1-N2	141.6(3)	O9-Dy3-O5	111.3(3)	O5-Dy5-O32	86.3(4)
O3-Dy1-O15	75.1(3)	O21-Dy3-O29	78.6(3)	O5-Dy5-O7	152.1(3)
O3-Dy1-O23	67.2(3)	O21-Dy3-O8	85.9(4)	O5-Dy5-O31	84.6(3)
O3-Dy1-O25	79.4(5)	O21-Dy3-O22	77.8(3)	O5-Dy5-N3	139.8(4)
O3-Dy1-O24	80.5(3)	O21-Dy3-O16	98.0(4)	O5-Dy5-O28	119.5(3)
O3-Dy1-O26	129.6(4)	O21-Dy3-O5	143.9(3)	O32-Dy5-O29	73.4(3)
O3-Dy1-O2	133.6(3)	O8-Dy3-O29	68.6(3)	O32-Dy5-O30	132.3(5)
O3-Dy1-O27	141.8(4)	O8-Dy3-O5	68.4(3)	O32-Dy5-O7	73.4(4)
O3-Dy1-N2	70.5(3)	O22-Dy3-O29	143.1(3)	O32-Dy5-O31	79.8(4)
O25-Dy1-O23	138.8(4)	O22-Dy3-O8	136.5(3)	O32-Dy5-N3	133.6(4)
O25-Dy1-O24	146.9(5)	O22-Dy3-O5	138.3(3)	O32-Dy5-O28	79.4(4)
O25-Dy1-O26	52.2(5)	O4-Dy3-O29	132.8(3)	O7-Dy5-O29	121.5(3)
O25-Dy1-N2	76.0(5)	O4-Dy3-O9	82.1(3)	O7-Dy5-O30	95.7(5)
O24-Dy1-O23	50.5(3)	O4-Dy3-O21	147.1(3)	O7-Dy5-O31	73.3(3)
O24-Dy1-N2	72.6(4)	O4-Dy3-O8	112.4(3)	O7-Dy5-N3	64.3(3)
O26-Dy1-O23	142.4(4)	O4-Dy3-O22	70.2(3)	O7-Dy5-O28	76.1(3)
O26-Dy1-O24	148.3(4)	O4-Dy3-O16	82.3(4)	O31-Dy5-O29	142.5(4)
O26-Dy1-N2	105.3(4)	O4-Dy3-O5	68.7(3)	O31-Dy5-N3	104.4(4)
O2-Dy1-O23	123.3(3)	O16-Dy3-O29	78.5(3)	O31-Dy5-O28	146.7(3)

O2-Dy1-O25	97.0(5)	O16-Dy3-O8	145.5(3)	N3-Dy5-O29	113.1(3)
O2-Dy1-O24	78.5(4)	O16-Dy3-O22	77.2(4)	O28-Dy5-O29	51.3(3)
O2-Dy1-O26	72.7(4)	O16-Dy3-O5	90.5(4)	O28-Dy5-N3	72.9(4)
O2-Dy1-N2	63.9(3)	O14-Dy4-O13	68.5(3)	O12-Dy6-O33	78.2(5)
O27-Dy1-O23	74.9(4)	O14-Dy4-O22	69.0(3)	O12-Dy6-O34	123.0(5)
O27-Dy1-O25	131.1(5)	O14-Dy4-O10	112.0(4)	O12-Dy6-O36	72.8(6)
O27-Dy1-O24	79.3(4)	O14-Dy4-O19	81.7(4)	O12-Dy6-N5	65.2(4)
O27-Dy1-O26	79.6(4)	O14-Dy4-O20	147.0(4)	O12-Dy6-O35	97.9(7)
O27-Dy1-O2	72.6(4)	O14-Dy4-O34	131.6(3)	O13-Dy6-O12	134.8(4)
O27-Dy1-N2	131.7(4)	O9-Dy4-O14	81.9(3)	O13-Dy6-O10	74.9(4)
N2-Dy1-O23	112.3(4)	O9-Dy4-O13	111.2(4)	O13-Dy6-O33	80.2(4)
O17-Dy2-O15	145.8(4)	O9-Dy4-O22	70.1(3)	O13-Dy6-O37	140.3(5)
O17-Dy2-O22	76.4(4)	O9-Dy4-O10	68.2(3)	O13-Dy6-O34	66.7(4)
O17-Dy2-O23	79.1(4)	O9-Dy4-O19	145.6(4)	O13-Dy6-O36	129.5(5)
O17-Dy2-O3	88.9(4)	O9-Dy4-O20	81.1(3)	O13-Dy6-N5	70.6(4)
O14-Dy2-O17	146.0(4)	O9-Dy4-O34	133.4(4)	O13-Dy6-O35	77.7(6)
O14-Dy2-O15	68.2(3)	O13-Dy4-O10	68.4(4)	O10-Dy6-O12	149.9(4)
O14-Dy2-O22	70.1(4)	O13-Dy4-O34	67.8(4)	O10-Dy6-O33	118.9(5)
O14-Dy2-O4	82.6(3)	O22-Dy4-O13	136.7(3)	O10-Dy6-O37	85.2(4)
O14-Dy2-O23	133.0(3)	O22-Dy4-O10	137.5(3)	O10-Dy6-O34	67.9(4)
O14-Dy2-O3	111.5(4)	O22-Dy4-O34	144.0(4)	O10-Dy6-O36	83.3(5)
O14-Dy2-O18	82.3(4)	O19-Dy4-O13	90.3(5)	O10-Dy6-N5	140.9(4)
O22-Dy2-O15	137.5(4)	O19-Dy4-O22	75.9(4)	O10-Dy6-O35	81.9(6)
O22-Dy2-O23	144.0(3)	O19-Dy4-O10	146.2(4)	O33-Dy6-O34	51.0(3)
O22-Dy2-O3	136.0(3)	O19-Dy4-O20	97.0(5)	O33-Dy6-N5	72.6(4)
O4-Dy2-O17	80.6(4)	O19-Dy4-O34	78.8(5)	O37-Dy6-O12	73.1(4)
O4-Dy2-O15	112.4(4)	O20-Dy4-O13	144.5(4)	O37-Dy6-O33	80.1(4)
O4-Dy2-O22	69.1(3)	O20-Dy4-O22	78.6(4)	O37-Dy6-O34	74.1(4)

O4-Dy2-O23	131.6(3)	O20-Dy4-O10	87.5(5)	O37-Dy6-O36	80.1(6)
O4-Dy2-O3	67.6(3)	O20-Dy4-O34	79.5(4)	O37-Dy6-N5	133.6(4)
O4-Dy2-O18	145.9(3)	O34-Dy4-O10	69.0(4)	O37-Dy6-O35	133.5(6)
O23-Dy2-O15	68.7(4)	O8-Dy5-O29	67.6(3)	O36-Dy6-O33	148.6(4)
O3-Dy2-O15	69.2(3)	O8-Dy5-O30	79.9(4)	O36-Dy6-O34	142.5(5)
O3-Dy2-O23	68.5(3)	O8-Dy5-O5	73.9(3)	O36-Dy6-N5	105.0(6)
O18-Dy2-O17	95.5(4)	O8-Dy5-O32	140.5(4)	O36-Dy6-O35	54.1(6)
O18-Dy2-O15	89.9(4)	O8-Dy5-O7	133.6(3)	N5-Dy6-O34	112.5(4)
O18-Dy2-O22	77.0(4)	O8-Dy5-O31	130.1(4)	O35-Dy6-O33	144.1(5)
O18-Dy2-O23	79.7(4)	O8-Dy5-N3	70.5(3)	O35-Dy6-O34	137.9(6)
O18-Dy2-O3	146.5(3)	O8-Dy5-O28	81.3(3)	O35-Dy6-N5	73.6(5)

Table S6. *SHAPE* analysis of the Dy(III) in cluster ***R*-1**.

Label	**Shape**	**Symmetry**	**Distortion** (°) **Dy1**
EP-9	D_{9h}	Enneagon	31.276
OPY-9	C_{8v}	Octagonal pyramid	22.208
HBPY-9	D_{7h}	Heptagonal bipyramid	17.232
JTC-9	C_{3v}	Triangular cupola J3	13.715
JCCU-9	C_{4v}	Capped cube (J8)	6.443
CCU-9	C_4	Capped cube	5.697
JCSAPR-9	C_{4v}	Capped sq. antiprism	1.838
CSAPR-9	C_{4v}	Capped square antiprism	1.251
JTCTPR-9	D_{3h}	Tricapped trigonal prism J51	2.101
TCTPR-9	D_{3h}	Tricapped trigonal prism	2.639
JTDIC-9	C_{3v}	Tridiminished icosahedron J63	13.695
HH-9	C_{2v}	Hula-hoop	10.544
MFF-9	C_s	Muffin	1.910

Table S7. *SHAPE* analysis of the Dy(III) in cluster ***S*-1**.

Label	Shape	Symmetry	Distortion (°)
			Dy1
EP-9	D_{9h}	Enneagon	31.265
OPY-9	C_{8v}	Octagonal pyramid	22.215
HBPY-9	D_{7h}	Heptagonal bipyramid	17.189
JTC-9	C_{3v}	Triangular cupola J3	13.721
JCCU-9	C_{4v}	Capped cube (J8)	6.410
CCU-9	C_4	Capped cube	5.651
JCSAPR-9	C_{4v}	Capped sq. antiprism	1.854
CSAPR-9	C_{4v}	Capped square antiprism	1.257
JTCTPR-9	D_{3h}	Tricapped trigonal prism J51	2.127
TCTPR-9	D_{3h}	Tricapped trigonal prism	2.635
JTDIC-9	C_{3v}	Tridiminished icosahedron J63	13.725
HH-9	C_{2v}	Hula-hoop	10.488
MFF-9	C_s	Muffin	1.918

Table S8. *SHAPE* analysis of the Dy(III) in cluster ***R*-2**.

Label	Shape	Symmetry	Distortion (°)		
			Dy1	Dy5	Dy6
EP-9	D_{9h}	Enneagon	35.677	35.638	35.343
OPY-9	C_{8v}	Octagonal pyramid	20.504	20.900	21.066
HBPY-9	D_{7h}	Heptagonal bipyramid	17.995	17.880	18.750
JTC-9	C_{3v}	Triangular cupola J3	15.084	15.463	15.299
JCCU-9	C_{4v}	Capped cube (J8)	10.650	10.149	10.407
CCU-9	C_4	Capped cube	9.947	9.873	9.580
JCSAPR-9	C_{4v}	Capped sq. antiprism	2.073	1.910	2.008
CSAPR-9	C_{4v}	Capped square antiprism	1.739	1.611	1.674
JTCTPR-9	D_{3h}	Tricapped trigonal prism J51	3.108	3.085	3.045

TCTPR-9	D_{3h}	Tricapped trigonal prism	2.473	2.463	2.415
JTDIC-9	C_{3v}	Tridiminished icosahedron J63	11.714	12.421	12.310
HH-9	C_{2v}	Hula-hoop	10.435	10.725	10.769
MFF-9	C_s	Muffin	1.947	1.740	1.718

Label	**Shape**	**Symmetry**	**Distortion** (°)		
			Dy2	**Dy3**	**Dy4**
OP-8	D_{8h}	Octagon	29.895	29.507	29.596
HPY-8	C_{7v}	Heptagonal pyramid	23.516	23.546	23.590
HBPY-8	D_{6h}	Hexagonal bipyramid	16.376	15.905	16.049
CU-8	O_h	Cube	12.862	12.534	12.399
SAPR-8	D_{4d}	Square antiprism	2.644	2.423	2.295
TDD-8	D_{2d}	Triangular dodecahedron	2.198	2.083	2.019
JGBF-8	D_{2d}	Johnson-Gyrobifastigium (J26)	13.118	13.381	12.966
JETBPY-8	D_{3h}	Johnson-Elongated triangular bipyramid (J14)	27.665	27.999	28.239
JBTP-8	C_{2v}	Johnson-Biaugmented trigonal prism (J50)	2.124	2.190	2.095
BTPR-8	C_{2v}	Biaugmen tedtrigonal prism	1.672	1.716	1.625
JSD-8	D_{2d}	Snub disphenoid (J84)	3.981	4.006	4.041
TT-8	T_d	Triakis tetrahedron	13.565	13.308	13.083
ETBPY-8	D_{3h}	Elongated trigonal bipyramid	24.777	24.417	24.196

Table S9. *SHAPE* analysis of the Dy(III) in cluster ***S*-2**.

Label	**Shape**	**Symmetry**	**Distortion** (°)		
			Dy1	**Dy5**	**Dy6**
EP-9	D_{9h}	Enneagon	35.497	35.314	35.505
OPY-9	C_{8v}	Octagonal pyramid	20.628	21.020	21.014
HBPY-9	D_{7h}	Heptagonal bipyramid	17.936	18.806	18.042
JTC-9	C_{3v}	Triangular cupola J3	15.120	15.211	15.323

JCCU-9	C_{4v}	Capped cube (J8)	10.694	10.386	10.218
CCU-9	C_4	Capped cube	9.890	9.532	9.983
JCSAPR-9	C_{4v}	Capped sq. antiprism	2.099	2.042	1.853
CSAPR-9	C_{4v}	Capped square antiprism	1.800	1.696	1.593
JTCTPR-9	D_{3h}	Tricapped trigonal prism J51	3.129	3.012	3.027
TCTPR-9	D_{3h}	Tricapped trigonal prism	2.546	2.403	2.427
JTDIC-9	C_{3v}	Tridiminished icosahedron J63	11.827	12.208	12.361
HH-9	C_{2v}	Hula-hoop	10.454	10.742	10.777
MFF-9	C_s	Muffin	1.983	1.745	1.723

Label	**Shape**	**Symmetry**	**Distortion** (°)		
			Dy2	**Dy3**	**Dy4**
OP-8	D_{8h}	Octagon	29.871	29.410	29.665
HPY-8	C_{7v}	Heptagonal pyramid	23.539	23.641	23.693
HBPY-8	D_{6h}	Hexagonal bipyramid	16.404	16.010	15.838
CU-8	O_h	Cube	12.858	12.349	12.489
SAPR-8	D_{4d}	Square antiprism	2.619	2.291	2.475
TDD-8	D_{2d}	Triangular dodecahedron	2.171	1.991	2.070
JGBF-8	D_{2d}	Johnson-Gyrobifastigium (J26)	13.111	13.004	13.296
JETBPY-8	D_{3h}	Johnson-Elongated triangular bipyramid (J14)	27.790	28.196	27.866
JBTP-8	C_{2v}	Johnson-Biaugmented trigonal prism (J50)	2.157	2.112	2.190
BTPR-8	C_{2v}	Biaugmen tedtrigonal prism	1.666	1.643	1.696
JSD-8	D_{2d}	Snub disphenoid (J84)	3.965	4.104	4.024
TT-8	T_d	Triakis tetrahedron	13.569	13.041	13.286
ETBPY-8	D_{3h}	Elongated trigonal bipyramid	24.659	24.230	24.442